



Synthesis and analytical characterization of Ca-BTC metal organic framework

Munazza Ramzan^a, Malika Rani^{a,*}, Rabia Siddiqui^a, Aqeel Ahmad Shah^b, Maryam Arshad^c, Muhammad Wasif Ghauri^d, Ghazanfar Abbas^d, Kareem Yusuf^e, Mika Sillanpää^f

^a Department of Physics, The Women University Multan, 66000, Pakistan

^b Department of Metallurgical Engineering, NED University of Engineering and Technology, Karachi, Pakistan

^c Cancer Genetics and Epigenetics Lab, Department of Biosciences, COMSATS University, Islamabad, Pakistan

^d Department of Physics, COMSATS University Islamabad, Lahore Campus, Pakistan

^e Department of Chemistry, College of Science, King Saud University, Riyadh 11451, Saudi Arabia

^f Department of Biological and Chemical Engineering, Aarhus University, Norrebrogade 44, 8000 Aarhus C, Denmark

ARTICLE INFO

Keywords:

Hydrothermal technique
XRD
SEM
EDS
FTIR
Raman spectroscopy
Photoluminescence
Zeta potential

ABSTRACT

Metal Organic framework (MOF) has been a class of great interest during the past few years owing to its decidedly applicative, easily synthesized and improved characteristics. Ca-BTC MOF is synthesized by Hydrothermal technique and reported for the first time. Its structural morphology was analyzed using XRD, SEM, and EDS, showing the tetragonal crystal structure having grain size of 24.92 nm and purity of sample respectively. FTIR, Raman Spectroscopy ensures the metal organic framework between Calcium and the tri-carboxylic group. Photoluminescence measures the energy gap of 3.792 eV, showing approximately the semiconducting behavior of synthesized material. Zeta potential having value of -13.5 mV confirms the instability having good microbial activity and conductivity i.e. 0.290 mS/cm which reveals important insights into its electrical properties.

1. Introduction

Metal-Organic-Frameworks, constructed from ions and Organic Ligands are known from 1980s. Metal-Organic-framework (MOF) known as Coordination Polymers within the realm of material science. Zeolites due to their micro porous structure, frequently compared to MOF. Due to the MOF wide variety in term of potential grafting [1,2], porous diameter [3] and Chemical composition Zeolites must concede to MOF.

The novelty of this study in the focused investigation of Ca-BTC, a specific MOF, and its comprehensive analytical characterization. This research advances in the field by providing detailed insights into the synthesis and properties of Ca-BTC, contributing to the broader understanding of MOFs and their potential applications.

MOFs have garnered significant attention in recent years due to their diverse range of applications, including enzymes immobilization [4–6] and separations [7], gas storage [8], Controlled discharge [9] or sensor [10]. Actually MOF are Crystalline materials in which atom or ions are Linked by Organic Linkers. Due to their attainable surface area and permanent permeable MOFs have gained

* Corresponding author.

E-mail address: dr.malikarani@wum.edu.pk (M. Rani).

<https://doi.org/10.1016/j.heliyon.2023.e21314>

Received 19 September 2023; Received in revised form 17 October 2023; Accepted 19 October 2023

Available online 20 October 2023

2405-8440/© 2023 The Authors. Published by Elsevier Ltd. This is an open access article under the CC BY-NC-ND license (<http://creativecommons.org/licenses/by-nc-nd/4.0/>).

great reorganization in the recent years [11–14]. Metal organic framework have inflated rank of Crystallinity and it is fascinating class of penetrable material, and have very high Permeability (50–90 %). And its surface area is extremely high (1000–8000 m²/g). The other name of Metal organic framework is PCP stands for porous coordination polymers [15–17] Adsorption of water [18], removal of toxic gas [19], storage of energy [20], sensing of chemical [21,22] Nano fluids [23,24] are broad range of applications of Metal organic framework. Analogous to the case of Zeolite, in industrial application the use of MOF powder often results in problems of Pressure drop. MOFs have captivated vast scientific attention during the past 10 years, that can be notice from expanding publications dedicated to this field and the other name of MOF is (PCPs) Porous Coordination Polymers [25]. They have magnificent physical properties and also can be described as multifunctional materials [26,27]. And MOFs Behave as hosts for many molecules. A MOFs continue to find relevance in industrial and environmental context, several challenges related to precursor availability, cost, and synthesis conditions need to be addressed [28]. In response, researchers have been exploring alternative and sustainable approaches for MOFs synthesis, including the use of waste-derived resources [29]. Recently, the development of MOFs based on alkaline earth metals, such as calcium, has gained traction [30]. Surface area reported in some MOF have exceed 500 m²g⁻¹ such as MIL-101 UCMC-1. Some MOFs reported in the literature with Surface area greater then 1000 m²g⁻¹ [31,32]. Metal centers and Organic linkers, these are the two main components of MOF. In MOF architecture one is Organic Secondary building unit while other is inorganic SBU. In organic SBU act as joints, while organic SBU act as the “struts” [33,34]. By the coordination of bonds these two components are connected to each other. On the other hand metal centers are metal Clusters in the MOF structure [35,36] they are rod-shaped clusters Sometimes [34]. By Organic linkers in MOF, Metal nodes are connected in a Crystalline network. And they have typically larger surface area [5,15,17]. At present 500,000 MOFs are predicted and 90,000 MOFs have been synthesized. In fact we have a increasing number of many MOFs [37–40], that have Vast range of application opens many route for research, and they are ready to be tested [3,33]. Target drug delivery [41], Magnetic networks [42], gas storage and Sequestrations [43,44], sensing [21,45], polymerization [46,47], luminescence [48,49], non-linear optics [50], magnetic networks, these are the technologically important applications of MOFs properties. To Clean polluted water (MOF) Metal organic framework [51–53] have exposed recently as very strong functional elements and to neutralize the adverse influence of human actions on the efficiency of earths water. Metal organic framework go in a direction to better utilization of fresh-water [54]. MOF used as absorptive of organic and in organic pollutants exist in water [55–58].

Using pattern of construction and functionalization of the skeleton, Metal organic framework structures are especially multitalented [15,59,60]. MOF are identified by the crystalline structure and have large surface area [61–63], functionalities and thermally stable. With different pore size and shape Mofs have become the versatile class, and attachment of variety of metals to various poly-complexing linkers like (sulfonates, phosphonates, carboxylates, imidazolates) are cause of discovery of many MOFs [63]. Bipyridyl and carboxylate-based molecule are the common liagands that have been involved in MOFs. Metal organic framework have easily tunable composition. Experimentally determined, with good accuracy potential to computationally predict, guests affinities for the emcee framework points to predesigned framework to provide required properties [64,65].

In the context of this research, we focus on the synthesis and analytical characterization of a specific MOF, Ca-BTC, elucidating its properties and characterization outcomes. Employing the Hydrothermal synthesis, we successfully prepared Ca-MOF, the synthesis of which is detailed in Fig. 1. The choice of calcium (Ca) as the metal center for building the Ca-BTC (Calcium Benzene-1,3,5-tricarboxylate) MOF in this research is that Calcium is a relatively abundant and cost-effective metal. Its use in MOFs may be advantageous for applications involving biological interactions, such as drug delivery or microbial studies, as it is less likely to introduce toxic effects. It can form stable coordination bonds with organic ligands like benzene-1,3,5-tricarboxylic acid (BTC). It allows for

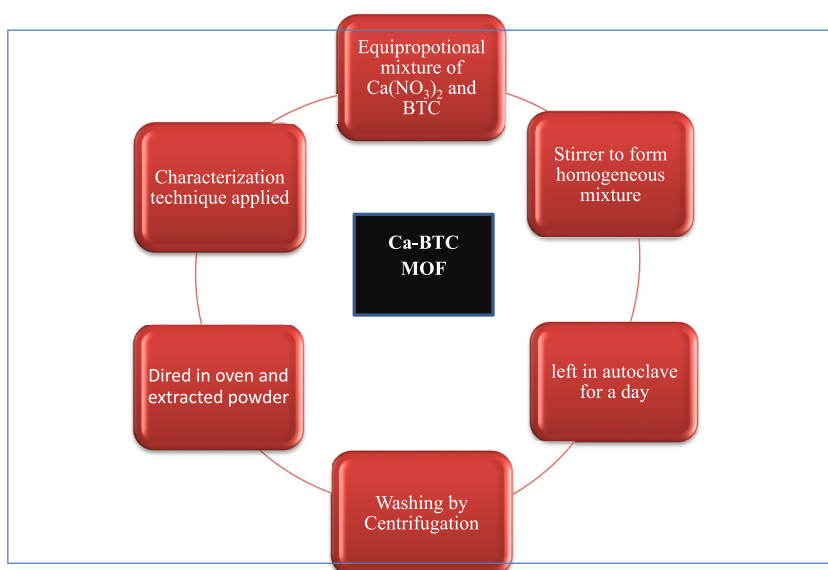


Fig. 1. Flow chart for the synthesis of Ca-BTC MOF.

controlled synthesis conditions and the formation of a desired MOF structure.

Structure, surface morphology, and electronic characteristics of Ca-MOF were analyzed by using the X-Ray Spectroscopy, SEM, Raman Spectroscopy, and Energy Dispersive X-ray Spectroscopy, Photoluminescence, Zeta Potential and FTIR spectroscopy.

In summary, this study not only adds to the growing body of knowledge concerning MOFs but also provides novel insights into the synthesis and characterization of Ca-BTC. By exploring the properties and potential applications of this specific MOF, we aim to bridge existing gaps in our understanding and inspire further research in this multifaceted field.

2. Details of the EXPERIMENTAL procedure

2.1. Chemical reagents

Calcium Nitrate $\text{Ca}(\text{NO}_3)_2 \cdot 4\text{H}_2\text{O}$, Trimesic acid [(95 %) pure Benzene-1,3,5-tricarboxylic acid, TMA, H3BTC or BTC] and Ethanol Absolute were brought from Sigma Aldrich and were used without any further purification. Distilled water was used as solvent. Ethanol was used for washing.

2.2. SYNTHESIS of Ca-BTC MOF

Ca-MOF was synthesized by hydrothermal technique mixture was allowed to self-organize in an autoclave for a day. (0.50g), Trimesic acid and (0.5g) of Calcium nitrate were added in 60 ml Distilled Water. After stirring of 15 min using magnetic stirrer the mixture was poured into steel-lined Teflon autoclave, which was then placed in DHG-9202 oven at 120°C for 12 h For self-processing. The sample was centrifuged at 6000 rpm for 3 times with Ethanol for the duration of 8 min. The sample was dried in an oven at 80°C overnight, then grinded using mortar and pestle to get nanoparticles. Obtained Ca-MOF powder was then undergone structural and optical characterization.

3. Results and discussion

3.1: X-Ray Diffraction (XRD):

Analysis shows the detail about the Sample's crystal structure and phase XRD pattern has 2θ ranges from 20 to 80 on x axis as shown in Fig. 2. For Ca-BTC MOF by comparing the peak with the standard peak of JCPDS file# 00-047-0703 we have evaluated major peaks of $2(\theta)$, main peaks of the XRD are at the point 30.24° , 38.45° , 41.15° , 44.68° , 65.07° , 72.65° and 78.16° on x axis. Our sample has tetragonal crystal structure indicating that it is extremely pure. Lattice parameters values of samples were shown that was 6.218 \AA and 11.0099 \AA representing a and c values respectively. And it has c/a ratio of >1 . Crystalline domain size was calculated for each peak independently.

3.1. 3.2: scanning electron microscopy (SEM)

SEM is one of the best scanning or testing instrument, for in situ examination of morphological dimension, for surface morphology and analysis of the particle size of Ca-MOF. Magnification at $20 \mu\text{m}$, $10 \mu\text{m}$, $1 \mu\text{m}$, $2 \mu\text{m}$, $5 \mu\text{m}$ has been shown for Ca-MOF in Fig. 3(a–e). These different magnifications showed that Ca-MOF possess regular crystalline layered structure. Small particle aggregated on the crystals are the unreacted content which were later removed by washing [66–68].

Fig. 3 clearly shows the morphological structure, distribution and agglomeration of the particles of Ca-MOF. The average grain size

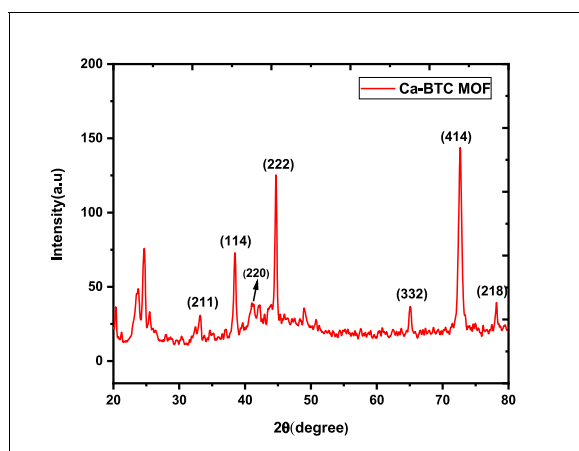


Fig. 2. XRD pattern of Ca-BTC MOF with hkl planes.

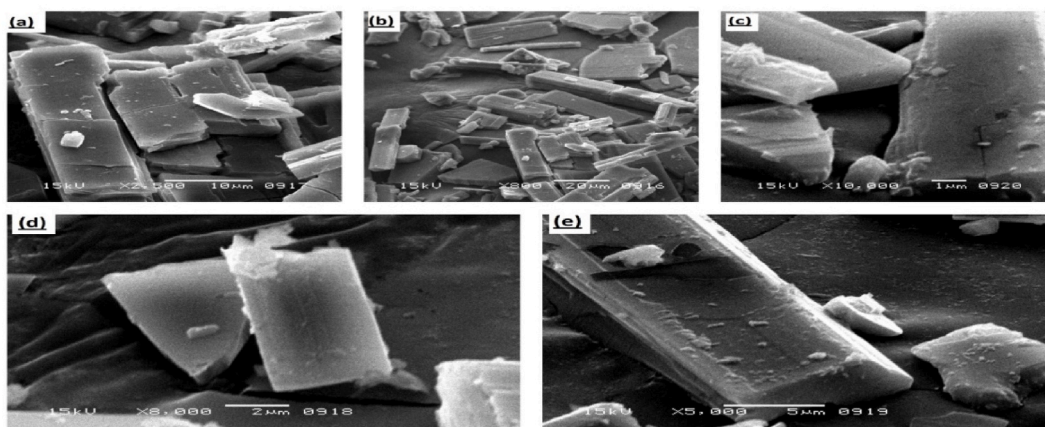


Fig. 3. SEM images of Ca-BTC MOF.

calculated is 24.92 nm, using the formula:

$$\text{Average grain size} = \frac{\text{Length of line}}{\text{Number of grains}}$$

3.2. 3.3: EDX analysis

Energy dispersive Analysis is sometimes referred to as “Energy Dispersive Spectroscopy (see Table 1). In very tiny sample of material primary approach for identifying and quantifying elemental composition is energy dispersive X-ray spectroscopy (EDS). In Table 2 ratios of Ca, C, O are given according to their atomic and weight ratios, showing the framework Calcium with tricarboxylic group. From EDS graph in Fig. 4(b) it is shown no extra impurity peaks appear its means our sample is pure and EDS graph showing novelty of our Work.

3.3. 4: fourier Transformation infrared spectroscopy (FTIR)

By using the FTIR spectra Surface functional groups of Calcium based metal organic framework were detected and demonstrated in Fig. 5. FTIR spectra shows many peaks in the range of 0–4500 cm^{-1} , and these peaks are at points of 3437 cm^{-1} O–H stretching via hydrogen bonding with water and CaO. 2922 cm^{-1} and 2511 cm^{-1} represents C–H and –COOH stretching respectively. The region from 1700 cm^{-1} to 1254 cm^{-1} relates to -O–C–O asymmetric and symmetric stretching of carboxylic acid, while peaks at 870 cm^{-1} Ca–H, 757 cm^{-1} shows Ca–H and Ca–O stretching mode of vibrations, which confirms the organic framework of development of Ca-MOF [69].

3.3.1. 5: Raman Spectroscopy

Raman spectra for Calcium based Metal organic framework in Fig. 6 lies in the region between 600 and 1800 cm^{-1} . Spectra showing the strong peak at 785 cm^{-1} and 996 cm^{-1} specifies the presence of Ca–O stretching as the part of calcium oxide cluster. Some other prominent peaks are at the point of 1706 cm^{-1} , 1593 cm^{-1} , 1405 cm^{-1} relate to O–C–O stretch with tridentate bridge owing to ionic carbonyl bond.

3.3.1.1. 6: photoluminescence (PL). Spectroscopy work by Capturing emitted light generated from the sample when an electron falls

Table 1

Crystalline size of Ca-BTC MOF.

2(θ) Values (degree)	θ Values (degree)	<i>hkl</i> values or miller indices	Intensity peak FWHM or (β) values in (radian)	Crystalline size of nanocomposite (D) nm	D(nm) Average
33.23757	16.618785	211	0.29654	27.93872735	18.01286
38.44989	0.38108	114	0.44001	19.11332851	
41.15367	20.576835	220	7.07949	1.210068676	
44.68193	22.34097	222	0.41532	20.6714854	
65.07325	32.53663	332	0.40098	23.49143858	
72.65867	36.32934	414	0.66925	14.72868239	
78.16661	39.08331	218	0.54026	18.93627609	

Table 2
Atomic and Weight ratios of Ca-BTC MOF.

Element	Weight %	Atomic%
Ca	11.01	4.02
C	48.31	58.81
O	40.67	37.17

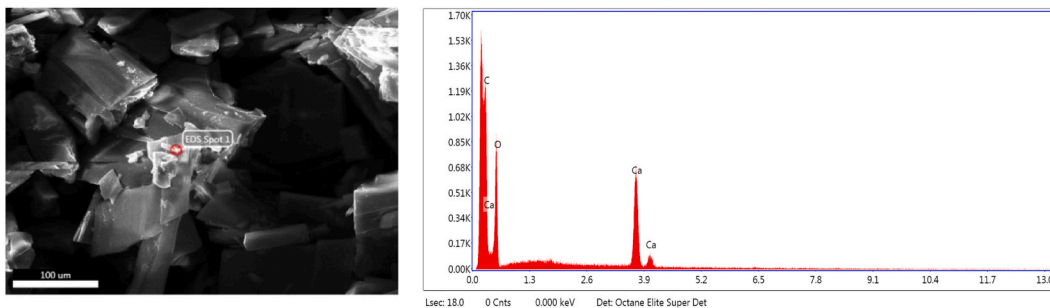


Fig. 4. (a): Surface morphology of Ca-BTC MOF (b): EDS spectra for Ca-BTC MOF.

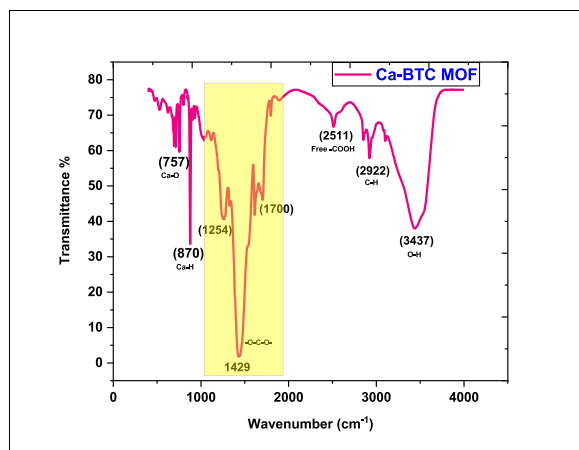


Fig. 5. FTIR spectra of Ca-BTC MOF.

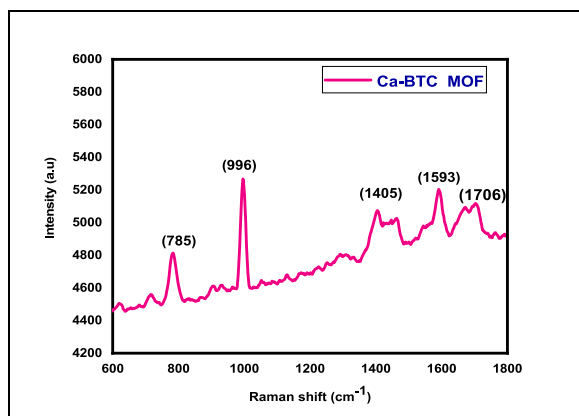


Fig. 6. Raman spectra of Ca-BTC MOF

from excited state to ground state when expose to a laser beam. Fig. 7 shows the maximum intensity peak is at 326.99 nm inside the visible spectrum. 2nd peak is because of some defects in the crystal structure. Energy band gap is calculated for highest intensity peak is using the formula: $E = \frac{hc}{\lambda} = \frac{1240}{\lambda} eV$.

3.4. 3.8: zeta potential

When materials diffuse in non-polar or in polar medium an important parameter related to its surface charge called zeta potential. The surface Zeta potential values are (ZPVs) of Ca-BTC MOF are given in Fig. 8, that showed highly negative charge with good colloidal stability because of its repulsive forces, which prevent the agglomeration of the nanoparticles. In the context of zeta potential analysis, the stability of Ca-BTC (Calcium Benzene-1,3,5-tricarboxylate) MOF can be assessed based on the surface charge characteristics and colloidal stability.

The zeta potential (ZPV) of -13.5 mV indicates that the Ca-BTC MOF surface carries a negative charge. Zeta potential is a crucial parameter in colloidal science because it provides insights into the electrostatic interactions between particles in a dispersion. A higher absolute value of zeta potential (either positive or negative) typically suggests greater electrostatic repulsion between particles, which helps prevent their aggregation or agglomeration. In the case of Ca-BTC MOF, the highly negative ZPV indicates good colloidal stability due to the presence of strong repulsive forces among MOF nanoparticles.

The negative charge on the surface of Ca-BTC MOF creates repulsive forces between individual MOF particles. These repulsive forces counteract the attractive forces that could lead to particle aggregation or settling. As a result, the MOF nanoparticles are less likely to agglomerate and remain well-dispersed in the medium, contributing to their colloidal stability.

The zeta deviation of 4.32 mV and a conductivity of 0.290 mS/cm provide additional information about the Ca-BTC MOF. The zeta potential analysis of Ca-BTC MOF reveals important insights into its electrical properties. The measured ZPV of -13.5 mV indicates that the surface of Ca-BTC MOF carries a negative charge, which, in the context of colloidal stability, plays a crucial role. While the ZPV itself does not directly signify semiconducting behavior, it is indicative of the material's surface charge characteristics [70]. Semiconductor materials typically exhibit an intermediate level of electrical conductivity, falling between conductors and insulators. In the case of Ca-BTC MOF, its negative surface charge, reflected in the ZPV, suggests the presence of mobile charge carriers within the material [71]. This semiconducting behavior, while not explicitly determined through zeta potential analysis, aligns with the known properties of MOFs, which often possess semiconducting characteristics. Further detailed electrical and electronic studies are warranted to comprehensively confirm the semiconducting behavior of Ca-BTC MOF [72]. This conclusion emphasizes that zeta potential analysis provides valuable clues that align with the expected semiconducting properties of MOFs, encouraging further investigation. Zeta deviation measures the variability in zeta potential values among particles in the dispersion. A smaller zeta deviation suggests relatively uniform surface charge among particles. The conductivity value is an indirect indicator of the presence of a large energy gap, which can affect the electronic properties of the MOF [73].

The ZPV of -13.5 mV, while indicating slightly weaker stability compared to more strongly charged materials, is still suitable for certain applications, particularly microbial studies. The negative surface charge of the MOF may have specific interactions with microbial cells or components, making it valuable for microbiological research.

Thus, the zeta potential analysis of Ca-BTC MOF reveals that it carries a negative surface charge, which contributes to its colloidal stability by promoting electrostatic repulsion between MOF particles. While the zeta potential is not extremely high (indicating a weaker stability), it remains suitable for specific applications, such as microbial studies. The zeta deviation and conductivity values provide additional insights into the MOF's surface charge and electronic properties.

4. Conclusion

Ca-BTC MOF is synthesized by hydrothermal technique and reported for the first time. The synthesis of Ca-BTC (Calcium Benzene-1,3,5-tricarboxylate) MOF, like any chemical process, has its own set of advantages like controlled structure, high surface area, versatile properties, eco-friendly material, scalable material etc., having disadvantages like complex synthesis, purification challenges, kinetic of MOF formation can be sensitive to reaction conditions, and scaling up the synthesis of MOFs like Ca-BTC from laboratory scale to industrial scale can present challenges, including maintaining product quality and consistency. Innovative calcium-BTC metal organic framework synthesized by the hydrothermal technique by using Calcium nitrate and benzenetricarboxylate (1,3,5-BTC) organic linked cubic structure. The presence of tetragonal structure was proved by XRD peaks. SEM image of the sample indicates structure of Ca-BTC MOF ranging from approximately, $1 \mu\text{m}$ – $2 \mu\text{m}$, $5 \mu\text{m}$, $10 \mu\text{m}$, $20 \mu\text{m}$ diameters. FTIR and Raman analysis contributed to prove the formation of basic MOF structure by verifying the location of peaks. And photoluminescence (PL) spectrum was performed to observe the Energy band gap and its value was 3.792 eV. Huge wavelength bandwidth of the peak and massive energy gap was observed by PL spectrum of calcium MOF. Zeta potential values (ZPVs) of MOF showed good results (-13.5 mV). No extra impurity peaks were seen in EDS, EDS graph showing Ca, O, C peaks appearance, evidences the purity and novelty of work.

Data availability statement

Data included in article/supp. material references in article.

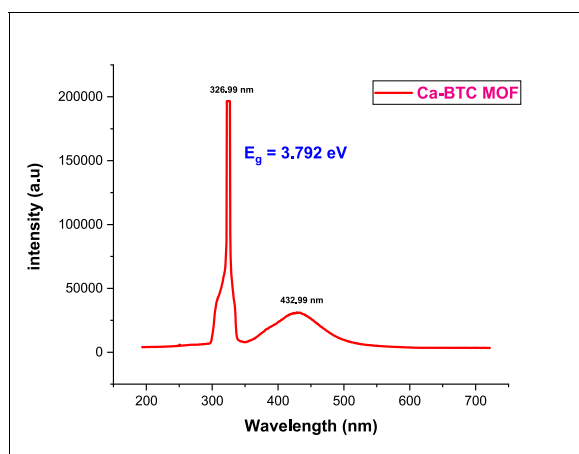


Fig. 7. PL Spectra of Ca-BTC MOF The energy band gap calculated is 3.792 eV. Bandwidth of PL spectrum of Ca-BTC MOF indicates attractive capability for photoluminescence application.

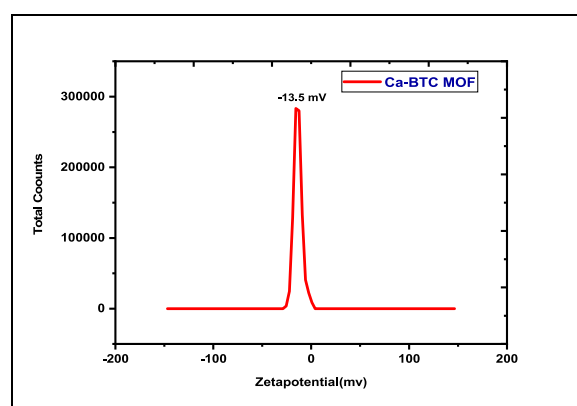


Fig. 8. Zeta potential for Ca-BTC MOF.

CRediT authorship contribution statement

Munazza Ramzan: Data curation, Formal Analysis, Investigation, Methodology, Visualization, Writing – original draft, Writing – review & editing, **Malika Rani:** Conceptualization, Data curation, Formal analysis, Funding acquisition, Investigation, Methodology, Project administration, Resources, Software, Supervision, Visualization, Validation, Writing - original draft, Writing - review & editing. **Rabia Siddiqui:** Data curation, Formal Analysis, Investigation, Methodology, Writing – original draft, Writing – review & editing, **Aqeel Ahmed Shah:** Data curation, Formal Analysis, Investigation, Methodology, Project administration, Resources, Software, Validation, Writing – review & editing, **Maryam Arshad:** Data curation, Formal Analysis, Investigation, Methodology, Project administration, Resources, Software, Validation, Writing – review & editing, **Muhammad Wasif Ghauri:** Data curation, Formal Analysis, Investigation, Methodology, Project administration, Resources, Software, Writing – review & editing, **Ghazanfar Abbas:** Data curation, Formal Analysis, Investigation, Methodology, Project administration, Resources, Software, Writing – review & editing, **Kareem Yusuf:** Data curation, Formal Analysis, Investigation, Resources, Methodology, Visualization, Writing – original draft, Writing – review & editing, **Mika Sillanpää:** Data curation, Formal Analysis, Investigation, Resources, Methodology, Visualization, Writing – original draft, Writing – review & editing.

Declaration of competing interest

The authors declare that they have no known competing financial interests or personal relationships that could have appeared to influence the work reported in this paper.

Acknowledgments

This work was funded by the Researchers Supporting Project Number (RSP2023R429) King Saud University, Riyadh, Saudi Arabia.

References

- [1] M. Savonnet, D. Bazer-Bachi, N. Bats, J. Perez-Pellitero, E. Jeanneau, V. Lecocq, C. Pinel, D. Farrusseng, Generic postfunctionalization route from amino-derived metal–organic frameworks, *Journal of the American Chemical Society* 132 (2010 March 16) 4518–4519, <https://doi.org/10.1021/ja909613e>.
- [2] S.M. Cohen, Postsynthetic methods for the functionalization of metal–organic frameworks, *Chem. Rev.* 112 (2012 September 14) 970–1000, <https://doi.org/10.1021/cr200179u>.
- [3] M. Eddaoudi, J. Kim, N. Rosi, D. Vodak, J. Wachter, M. O’Keeffe, O.M. Yaghi, Systematic design of pore size and functionality in isoreticular MOFs and their application in methane storage, *Science* 295 (2002) 469–472, <https://doi.org/10.1126/science.1067208>.
- [4] A. Corma, H.I. Garcia, F.X. Llabrés i Xamena, Engineering metal organic frameworks for heterogeneous catalysis, *Chemical reviews* 110 (April 1) (2010) 4606–4655, <https://doi.org/10.1021/cr9003924>.
- [5] J.Y. Lee, O.K. Farha, J. Roberts, K.A. Scheidt, S.B.T. Nguyen, J.T. Hupp, Metal–organic framework materials as catalysts, *Chem. Soc. Rev.* 38 (2009 March 17) 1450–1459, <https://doi.org/10.1039/B807080F>.
- [6] D. Farrusseng, S. Aguado, C. Pinel, Metal–organic frameworks: opportunities for catalysis, *Angewandte Chemie International Edition* 48 (September 23) (2009) 7502–7513, <https://doi.org/10.1002/anie.200806063>.
- [7] J.-R. Li, R.J. Kuppler, H.-C. Zhou, Selective gas adsorption and separation in metal–organic frameworks, *Chem. Soc. Rev.* 38 (2009 March 26) 1477–1504, <https://doi.org/10.1039/B802426J>.
- [8] L.J. Murray, M. Dincă, J.R. Long, Hydrogen storage in metal–organic frameworks, *Chem. Soc. Rev.* 38 (March 25) (2009) 1294–1314, <https://doi.org/10.1039/B802256A>.
- [9] P. Horcajada, C. Serre, M. Vallet-Regí, M. Sebban, F. Taulelle, G. Férey, Metal–organic frameworks as efficient materials for drug delivery, *Angewandte chemie* 118 (September 5) (2006) 6120–6124, <https://doi.org/10.1002/ange.200601878>.
- [10] G. Lu, J.T. Hupp, Metal–organic frameworks as sensors: a ZIF-8 based Fabry–Pérot device as a selective sensor for chemical vapors and gases, *J. Am. Chem. Soc.* 132 (2010) 7832–783311, <https://doi.org/10.1021/ja101415b>.
- [11] S.M. Cohen, Modifying MOFs: new chemistry, new materials, *Chemical Science*, 1 1 (1) (2010) 32–36, <https://doi.org/10.1039/C0SC00127A>.
- [12] G.J. Férey, Hybrid porous solids: past, present, future. *Chem. Soc. Rev.* 37 (September 19) (2008) 191–214, <https://doi.org/10.1039/B618320B>.
- [13] R.J. Kuppler, D.J. Timmons, Q.R. Fang, J.R. Li, T.A. Makal, M.D. Young, D. Yuan, D. Zhao, W. Zhuang, H.C. Zhou, Potential applications of metal-organic frameworks, *Coordination Chemistry Reviews* 253 (23–24) (2009 December) 3042–3066, <https://doi.org/10.1016/j.ccr.2009.05.019>.
- [14] H.L. Jiang, Q.J. Xu, Porous metal–organic frameworks as platforms for functional applications, *Chemical Communications* 47 (2011 February 02) 3351–3370, <https://doi.org/10.1039/C0CC05419D>.
- [15] H. Furukawa, K.E. Cordova, M. O’Keeffe, O.M. Yaghi, The chemistry and applications of metal-organic frameworks, *Science* 341 (2013), 1230444, <https://doi.org/10.1126/science.1230444>.
- [16] H. Furukawa, U. Müller, O.M. Yaghi, Heterogeneity within order, in metal–organic frameworks. *Angewandte Chemie International Edition* 54 (13) (2015 January) 3417–3430, <https://doi.org/10.1002/anie.201410252>.
- [17] H.-C. Zhou, J.R. Long, O.M. Yaghi, Introduction to metal–organic frameworks, *Chemical reviews* 112 (2012) 673–674, <https://doi.org/10.1021/cr300014x>.
- [18] J. Canivet, A. Fateeva, Y. Guo, B. Coasne, D. Farrusseng, Water adsorption in MOFs, fundamentals and applications 43 (May 29) (2014) 5594–5617, <https://doi.org/10.1039/C4CS00078A>.
- [19] E. Barea, C. Montoro, J.A. Navarro, Toxic gas removal–metal–organic frameworks for the capture and degradation of toxic gases and vapours, *Chem. Soc. Rev.* 43 (April 7) (2014) 5419–5430, <https://doi.org/10.1039/C3CS60475F>.
- [20] J.W. Jeon, R. Sharma, P. Meduri, B.W. Arey, H.T. Schaeff, J.L. Lutkenhaus, J.P. Lemmon, P.K. Thallapally, M.I. Nandasiri, B.P. McGrail, S.K. Nune, In situ one-step synthesis of hierarchical nitrogen-doped porous carbon for high-performance supercapacitors 6 (April 30) (2014) 7214–7222, <https://doi.org/10.1021/am500339x>.
- [21] Z. Hu, B.J. Deibert, J.J. Li, Luminescent metal–organic frameworks for chemical sensing and explosive detection, *Chem. Soc. Rev.* 43 (2014 February 28) 5815–5840, <https://doi.org/10.1039/C4CS00010B>.
- [22] L.E. Kreno, K. Leong, O.K. Farha, M. Allendorf, R.P. Van Duyne, J.T. Hupp, Metal–organic framework materials as chemical sensors 112 (2012 November 9) 1105–1125, <https://doi.org/10.1021/cr200324t>.
- [23] B.P. McGrail, P.K. Thallapally, J. Blanchard, S.K. Nune, J.J. Jenks, L.X. Dang, Metal-organic heat carrier nanofluids 2 (2013 September) 845–855, <https://doi.org/10.1016/j.nanoen.2013.02.007>.
- [24] H.V. Annapureddy, S.K. Nune, R.K. Motkuri, B.P. McGrail, L.X. Dang, A combined experimental and computational study on the stability of nanofluids containing metal organic frameworks, *J. Phys. Chem. B* 119 (January 8) (2015) 8992–8999, <https://doi.org/10.1021/jp5079086>.
- [25] N.W. Ockwig, O. Delgado-Friedrichs, M. O’Keeffe, O.M. Yaghi, Reticular chemistry: occurrence and taxonomy of nets and grammar for the design of frameworks, *Accounts of chemical research* 38 (3) (2005 January 19) 176–182, <https://doi.org/10.1021/ar020022l>.
- [26] X.M. Zhang, Z.M. Hao, W.X. Zhang, X.M. Chen, Dehydration-induced conversion from a single-chain magnet into a metamagnet in a homometallic nanoporous metal–organic framework 46 (April 27) (2007) 3456–3459, <https://doi.org/10.1002/ange.200604284>.
- [27] P. Moeck, Nano-tech/science education at a research university, in: *IEEE 13th Nanotechnology Materials and Devices Conference (NMDC)*, IEEE, 2018, pp. 1–6, <https://doi.org/10.1109/NMDC.2018.8605858>.
- [28] V. Somjit, P. Thinsoongnoen, S. Waiprasoet, T. Pila, P. Pattanasattayavong, S. Horike, K. Kongpatpanich, Processable UiO-66 metal–organic framework fluid gel and electrical conductivity of its nanofilm with sub-100 nm thickness, *ACS Appl. Mater. Interfaces* 13 (2021 June 24) 30844–30852, <https://doi.org/10.1021/acsmi.1c07262>.
- [29] H. Li, Y. Wang, Z. Han, T. Wang, Y. Wang, C. Liu, M. Guo, G. Li, W. Lu, M. Yu, X. Ma, Nanosheet like CaO/C derived from Ca-BTC for biodiesel production assisted with microwave, *Applied Energy* 326 (2022 November 15), 120045, <https://doi.org/10.1016/j.apenergy.2022.120045>.
- [30] R.M. Abdelhameed, S.F. Hammad, I.A. Abdallah, A. Bedair, M. Locatelli, F.R. Mansour, A hybrid microcrystalline cellulose/metal-organic framework for dispersive solid phase microextraction of selected pharmaceuticals: A proof-of-concept. *J. Pharm. Biomed. Anal.* 235 (2023 October 25), 115609, <https://doi.org/10.1016/j.jpba.2023.115609>.
- [31] G. Férey, C. Mellot-Draznieks, C. Serre, F. Millange, J. Dutour, S. Surblé, I. Margiolaki, A chromium terephthalate-based solid with unusually large pore volumes and surface area, *Science* 309 (September 23) (2005) 2040–2042, <https://doi.org/10.1126/science.1116275>.
- [32] Q.R. Fang, G.S. Zhu, Z. Jin, M. Xue, X. Wei, D.J. Wang, S.L. Qiu, A novel metal, Organic Framework with the Diamondoid Topology Constructed from Pentanuclear Zinc–Carboxylate Clusters 7 (2007 May 19) 1035–1037, <https://doi.org/10.1021/cg060829a>.
- [33] O.M. Yaghi, M. O’Keeffe, N.W. Ockwig, H.K. Chae, M. Eddaoudi, J. Kim, Reticular synthesis and the design of new materials 423 (2003 June 12) 705–714, <https://doi.org/10.1038/nature01650>.
- [34] A.R. Millward, O.M. Yaghi, Metal–organic frameworks with exceptionally high capacity for storage of carbon dioxide at room temperature, *J. Am. Chem. Soc.* 127 (2005) 17998–17999, <https://doi.org/10.1021/ja0570032>.
- [35] M. Dinca, A.F. Yu, J.R. Long, Microporous metal–organic frameworks incorporating 1, 4-benzeneditrazolate: syntheses, structures, and hydrogen storage properties, *J. Am. Chem. Soc.* 128 (2006 June 16) 8904–8913, <https://doi.org/10.1021/ja061716i>.
- [36] B. Chen, N.W. Ockwig, A.R. Millward, D.S. Contreras, O.M. Yaghi, High H₂ adsorption in a microporous metal–organic framework with open metal sites, *Angewandte Chemie* 44 (2005 July 18) 4745–4749, <https://doi.org/10.1002/ange.200462787>.
- [37] P.Z. Moghadam, A. Li, S.B. Wiggan, A. Tao, A.G. Maloney, P.A. Wood, S.C. Ward, D. Fairen-Jimenez, Development of a cambridge structural database subset, a collection of metal–organic frameworks for past, present, and future 29 (2017 March 14) 2618–2625, <https://doi.org/10.1021/acs.chemmater.7b00441>.
- [38] Y.G. Chung, E. Haldoupis, B.J. Bucior, M. Haranczyk, S. Lee, H. Zhang, K.D. Vogiatzis, M. Milisavljevic, S. Ling, J.S. Camp, B. Slater, Advances, updates, and analytics for the computation-ready, experimental metal–organic framework database: CoRE MOF 2019, *J. Chem. Eng. Data* 64 (November 4) (2019) 5985–5998, <https://doi.org/10.1021/acs.jced.9b00835>.

- [39] C.E. Wilmer, M. Leaf, C.Y. Lee, O.K. Farha, B.G. Hauser, J.T. Hupp, R.Q. Snurr, Large-scale screening of hypothetical metal–organic frameworks, *Nature Chem* 4 (2012 February) 83–89, <https://doi.org/10.1038/nchem.1192>.
- [40] P.G. Boyd, A. Chidambaram, E. García-Díez, C.P. Ireland, T.D. Daff, R. Bounds, A. Gładysiak, P. Schouwink, S.M. Moosavi, M.M. Maroto-Valer, J.A. Reimer, Data-driven design of metal–organic frameworks for wet flue gas CO₂ capture, *Nature* 576 (2019) 253–256, <https://doi.org/10.1038/nchem.1192>.
- [41] P. Horcajada, et al., Porous metal–organic-framework nanoscale carriers as a potential platform for drug delivery and imaging, *Nature Materials* 9 (13) (2010 December) 172–178, <https://doi.org/10.1038/nmat2608>.
- [42] M.J. Kurmoo, Magnetic metal–organic frameworks 38 (February 24) (2009) 1353–1379, <https://doi.org/10.1039/B804757J>.
- [43] J. Liu, P.K. Thallapally, B.P. McGrail, D.R. Brown, Progress in adsorption-based CO₂ capture by metal–organic frameworks, *Chem. Soc. Rev.* 41 (2012 December 5) 2308–2322, <https://doi.org/10.1039/C1CS15221A>.
- [44] Y. He, W. Zhou, G. Qian, B. Chen, Methane storage in metal–organic frameworks, *Chem. Soc. Rev.* 43 (2014 March 21) 5657–5678, <https://doi.org/10.1039/C4CS00032C>.
- [45] C.M.D.C. Serre, C. Mellot-Draznieks, S. Surblé, N. Audebrand, Y. Filinchuk, G. Férey, Role of solvent–host interactions that lead to very large swelling of hybrid framework, *Science* 315 (2007) 1828–1831, <https://doi.org/10.1126/science.1137975>.
- [46] T. Uemura, N. Yanai, S.J. Kitagawa, Polymerization reactions in porous coordination polymers, *Chem. Soc. Rev.* 38 (February 3) (2009) 1228–1236, <https://doi.org/10.1039/B802583P>.
- [47] M.J. Vitorino, T. Devic, M. Tromp, G. Férey, M. Visseaux, Lanthanide Metal–Organic Frameworks as Ziegler–Natta Catalysts for the Selective Polymerization of Isoprene, *Macromol. Chem. Phys.* 210 (2009 November 24) 1923–1932, <https://doi.org/10.1002/macp.200900354>.
- [48] M.D. Allendorf, C.A. Bauer, R.K. Bhakta, R.J.T. Houk, Luminescent metal–organic frameworks, *Chem. Soc. Rev.* 38 (January 27) (2009) 1330–1352, <https://doi.org/10.1039/B802352M>.
- [49] K.A. White, D.A. Chengelis, K.A. Gogick, J. Stehman, N.L. Rosi, S. Petoud, Near-infrared luminescent lanthanide MOF barcodes, *J. Am. Chem. Soc.* 131 (2009 November 25), <https://doi.org/10.1021/ja907885m>.
- [50] S. Bordiga, et al., K.–P, Lillerud, M. Bjorgen and A. Zecchina 20 (2004) 2300.
- [51] N.L. Rosi, M. Eddaoudi, J. Kim, M. O’Keeffe, O.M. Yaghi, Advances in the chemistry of metal–organic frameworks 4 (2002 July 19), <https://doi.org/10.1039/b203193k>.
- [52] K.E. Cordova, O.M. Yaghi, The ‘folklore’ and reality of reticular chemistry, *Mater. Chem. Front* 1 (2017 May 05), <https://doi.org/10.1039/C7QM00144D>.
- [53] H. Furukawa, K.E. Cordova, M. O’Keeffe, O.M. Yaghi, The chemistry and applications of metal–organic frameworks, *Science* 341 (2013 August 30), <https://doi.org/10.1126/science.1230444>.
- [54] L. Xu, Impact of Climate Change and Human Activity on the Eco-Environment: an Analysis of the Xisha Islands, Springer, 2014, <https://doi.org/10.1007/978-3-662-45003-1>.
- [55] I. Ahmed, T. Panja, N.A. Khan, M. Sarker, J.S. Yu, S.H. Jung, Nitrogen-doped porous carbons from ionic liquids@ MOF: remarkable adsorbents for both aqueous and nonaqueous media, *ACS Appl. Mater. Interfaces* 9 (2017 February 27), <https://doi.org/10.1021/acsami.7b00859>.
- [56] N.A. Khan, Z. Hasan, S.H. Jung, Adsorptive removal of hazardous materials using metal–organic frameworks (MOFs): a review, *J. Hazard. Mater* 244 (2013 January 15), <https://doi.org/10.1016/j.jhazmat.2012.11.011>.
- [57] E.M. Dias, C. Petit, Correction: Towards the use of metal–organic frameworks for water reuse: a review of the recent advances in the field of organic pollutants removal and degradation and the next steps in the field, *J. Mater. Chem. A* 4 (2015 September 25), <https://doi.org/10.1039/C5TA05440K>.
- [58] P.A. Kobielska, A.J. Howarth, O.K. Farha, S. Nayak, Metal–organic Frameworks for Heavy Metal Removal from Water, 2018 March 01, p. 358, <https://doi.org/10.1016/j.ccr.2017.12.010>.
- [59] C. Wang, D. Liu, W. Lin, Metal–organic frameworks as a tunable platform for designing functional molecular materials, *J. Am. Chem. Soc.* 135 (2013 August 14), <https://doi.org/10.1021/ja308229p>.
- [60] A. Bétard, R.A. Fischer, Metal–organic framework thin films: from fundamentals to application, *Chem. Rev* 112 (2012 February 08), <https://doi.org/10.1021/cr200167v>.
- [61] O.K. Farha, I. Eryazici, N.C. Jeong, B.G. Hauser, C.E. Wilmer, A.A. Sarjeant, R.Q. Snurr, S.T. Nguyen, A.O. Yazaydin, J.T. Hupp, Metal–organic framework materials with ultrahigh surface areas: is the sky the limit? *J. Am. Chem. Soc.* 134 (2012 August 20) <https://doi.org/10.1021/ja3055639>.
- [62] M. Eddaoudi, H. Li, O.M. Yaghi, Highly porous and stable metal–organic frameworks: structure design and sorption properties, *J. Am. Chem. Soc.* 122 (2000 February 04), <https://doi.org/10.1021/ja9933386>.
- [63] T. Han, C. Li, X. Guo, H. Huang, D. Liu, C. Zhong, In-situ synthesis of SiO₂@ MOF composites for high, efficiency removal of aniline from aqueous solution 390 (30) (2016 december), <https://doi.org/10.1016/j.apsusc.2016.08.111>.
- [64] O.K. Farha, A. Özgür Yazaydin, I. Eryazici, C.D. Malliakas, B.G. Hauser, M.G. Kanatzidis, S.T. Nguyen, R.Q. Snurr, J.T. Hupp, De novo synthesis of a metal–organic framework material featuring ultrahigh surface area and gas storage capacities 2 (2010 September 12), <https://doi.org/10.1038/nchem.834>.
- [65] P. Ryan, O.K. Farha, L.J. Broadbelt, R.Q. and Snurr, Computational screening of metal–organic frameworks for xenon/krypton separation 57 (2011), <https://doi.org/10.1002/aic.12397>.
- [66] M. Mazaj, N. Zabukovec Logar, Phase formation study of Ca-terephthalate MOF-type materials. *Crystal Growth & Design* 15 (2014 December 19), <https://doi.org/10.1021/cg501273b>.
- [67] S. Suprpto, T.R. Fauziah, M.S. Sangi, T.P. Oetami, I. Qoniah, D. Prasetyoko, Calcium oxide from limestone as solid base catalyst in transesterification of Reutealis trisperma oil. *Indonesian Journal of Chemistry* 16 (2016), <https://doi.org/10.22146/ijc.21165>.
- [68] Z.H.U. Huaping, W.U. Zongbin, C. Yuanxiong, P. Zhang, D.U.A. N Shijie, L.I. U Xiaohua, M.A.O. Zongqiang, Preparation of biodiesel catalyzed by solid super base of calcium oxide and its refining process, *Chin J Catal* 27 (2006 May), [https://doi.org/10.1016/S1872-2067\(06\)60024-7](https://doi.org/10.1016/S1872-2067(06)60024-7).
- [69] U. Jamil, A.H. Khoja, R. Liaquat, S.R. Naqvi, W.N.N.W. Omar, N.A.S. Amin, Copper and Calcium-Based Metal Organic Framework (MOF) Catalyst for Biodiesel Production from Waste Cooking Oil: A Process Optimization Study, *Energy Conversion and Management*, 215, 2020 July 01, <https://doi.org/10.1016/j.enconman.2020.112934>.
- [70] E. Moumen, L. Bazzi, S. El Hankari, Aluminum-fumarate based MOF, Aluminum-fumarate based MOF: A promising environmentally friendly adsorbent for the removal of phosphate. *Process Safety and Environmental Protection* 160 (2022 April) (2022), <https://doi.org/10.1016/j.psep.2022.02.034>.
- [71] A.J. Clough, N.M. Orchanian, J.M. Skelton, A.J. Neer, S.A. Howard, C.A. Downes, L.F. Piper, A. Walsh, B.C. Melot, S.C. Marinescu, Room temperature metallic Conductivity in a metal–organic framework Induced by oxidation, *J. Am. Chem. Soc.* 141 (2019 September 25) 16323–16330, <https://doi.org/10.1021/jacs.9b06898>.
- [72] M. Islamov, H. Babaei, R. Anderson, K.B. Sezginel, J.R. Long, A.J. McGaughey, D.A. Gomez-Gualdrón, High-throughput screening of hypothetical metal–organic frameworks for thermal conductivity, *npj Comput. Mater.* 9 (2023 January 20) 11, <https://doi.org/10.1038/s41524-022-00961-x>.
- [73] P. Bajpai, Chapter 10 - papermaking chemistry, in: P. Bajpai (Ed.), *Biermann’s Handbook of Pulp and Paper*, third ed., Elsevier, 2018, pp. 207–236.